Research Article | Vol. 26, No. 23 | 12 Nov 2018 | OPTICS EXPRESS 29916
Optics EXPRESS

Delta-sigma-modulated IFoF transmission system assisted by a correlative-level encoding technique

SEUNGHYUN JANG,[1,*] BONGHYUK PARK,[1] SONGCHEOL HONG,[2] KWANG-SEON KIM,[1] AND KWANG-CHUN LEE[1]

[1]*Giga-communication Research Group, Electronics and Telecommunications Research Institute, 218 Gajeongno, Yuseong-gu, Daejeon 305-700, South Korea*
[2]*Department of Electrical Engineering, Korea Advanced Institute of Science and Technology, 335 Gwahangno, Yuseong-gu, Daejeon 305-701, South Korea*
**damduk@etri.re.kr*

Abstract: A delta-sigma-modulated intermediate-frequency-over-fiber (IFoF) transmission system assisted by a correlative-level coding technique is proposed and experimentally demonstrated. Unlike conventional delta-sigma IFoF systems with multiple output levels to achieve higher signal quality or larger capacity, a correlative-level encoder is exploited as a second modulator preceded by the delta-sigma modulator. The encoder compresses the bandwidth of the delta-sigma modulated signal by creating a correlation between adjacent signal symbols. As a result, the sampling frequency of the delta-sigma modulator in the proposed system can be increased beyond the transmission bandwidth of the IFoF system, considerably improving the in-band signal quality and the transmission capacity over the conventional multi-level approach. This is because the quantization noise from the delta-sigma modulation in the proposed scheme is more aggressively pushed away from the signal bandwidth with the high sampling frequency. According to experimental results, the proposed link provides at least a 40% larger transmission capacity for similar in-band signal quality or 2.1% better average EVM performance for the same capacity than the conventional four-level pulse-amplitude-modulation delta-sigma IFoF systems.

1. Introduction

Analog radio-over-fiber systems have numerous advantages: low attenuation, simple architecture, modulation format transparency, and future proof. However, the performance of the systems is considerably affected by non-linearity and spectral impurity, which therefore limits their widespread use [1–5].

Recently, delta-sigma-digitized intermediate-frequency-over-fiber (IFoF) systems, as shown in Fig. 1, have been proposed and have attracted much attention as analog-signal transmission systems [5–12]. This is because robust digital transmission as a means of transporting analog signals is possible by converting the analog signals into digital pulse trains with delta-sigma modulation, while most of the advantages of the analog-based transmission are still provided. According to recent studies, to further harness the delta-sigma IFoF systems, multi-level approaches have been investigated to achieve larger capacity or better signal quality [8,9,12]. This is because the amount of quantization noise is inversely proportional to the number of quantization levels.

However, for the multi-level delta-sigma-digitized pulse train to be directly transported over an optical link, the number of quantization levels must be determined by considering the optical transmission signaling format, such as four-level pulse-amplitude modulation (PAM-4), and therefore is practically limited. Due to this practical limitation, the benefits gained by the multi-level approach are not significant. In addition, the sampling frequency of a delta-

#334766 https://doi.org/10.1364/OE.26.029916
Journal © 2018 Received 8 Jun 2018; revised 17 Sep 2018; accepted 7 Oct 2018; published 31 Oct 2018

Optics EXPRESS

sigma modulator for optical transmission, especially the mobile fronthaul, is extremely high, 10 GHz or above [8,9]. At such very high-frequency ranges, multi-amplitude-level non-linearity is not adequately compensated for due to the difficulty of implementing the compensation circuit, thereby significantly deteriorating the quality of the delta-sigma modulated signal.

In this paper, we propose a different approach to achieve the same goals. Rather than using a multi-level quantizer for the delta-sigma modulation, we exploit a correlative-level encoder as a post-modulation stage. The purpose of the additional block is to reduce the bandwidth of the delta-sigma-digitized pulse train. As a result, the sampling frequency of the delta-sigma modulator can be increased up to a frequency where the overall bandwidth of the two cascaded blocks of the delta-sigma modulator and the correlative encoder lies within the transmission bandwidth, and then the correlatively-coded delta-sigma pulse trains can be transmitted over the transmission link. With the proposed scheme, the capacity of the proposed IFoF system with a given transmission bandwidth is significantly enhanced because the quantization noise generated by the delta-sigma modulation is more dramatically shaped with the higher sampling frequency than in the multi-level approach. To verify the effectiveness of the proposed delta-sigma IFoF system, we conducted simulation and transmission experiments with two more conventional multi-level delta-sigma IFoF systems.

The remainder of this paper is organized as follows. Section 2 introduces the structure and the problems of the conventional delta-sigma IFoF system. Section 3 presents the proposed correlatively-coded delta-sigma IFoF system and explains the basic operation principle of the scheme. In Section 4, the experimental setup and evaluation results of the proposed and the conventional IFoF transmission systems are provided and discussed. Finally, the conclusions are described in Section 5.

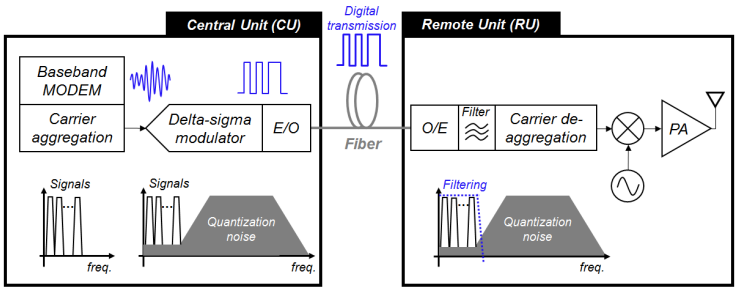

Fig. 1. Delta-sigma IFoF transmission system.

2. Conventional delta-sigma-IFoF systems

This section introduces the conventional delta-sigma modulations for IFoF systems and describes the limitation and problem of the conventional approach.

2.1 Conventional multi-level delta-sigma modulation

The operation principle of a conventional two-level delta-sigma modulation and its output power spectral density (PSD) are illustrated in Fig. 2. Because the maximum sampling frequency of the two-level delta-sigma modulator shown in the upper path in Fig. 2 is limited by the transmission rate of the system, to further improve the in-band signal quality or the capacity, a multi-level quantizer can be adopted. This is because the quantization noise power is

$$q_{total,RMS}^2 = \Delta^2 / 12, \tag{1}$$

Optics EXPRESS

where Δ is the least significant bit (LSB), and as the number of quantization levels increases, the quantization noise power decreases in proportion to the square of the number of levels. Therefore, most recent studies have exploited the multi-level approach [8,9,12].

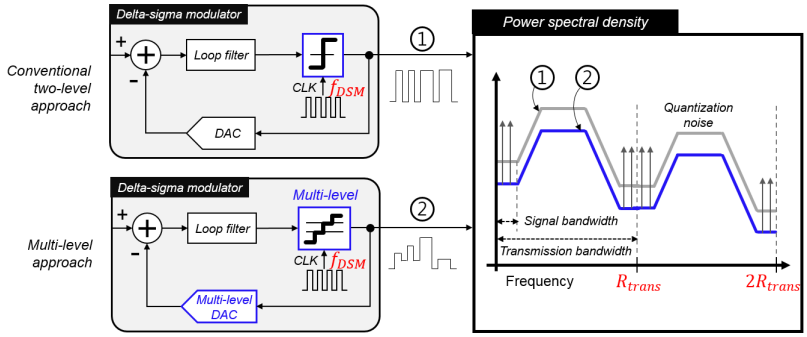

Fig. 2. Conventional delta-sigma modulations with two and multi-levels and an example of their output PSD.

2.2 Limitation and problem of the multi-level approach in IFoF transmission

However, because the output pulse train of the delta-sigma modulator is directly transported over the conventional IFoF link, the number of quantization levels cannot continue to increase and is limited at some level. Owing to the fact that PAM-4 is more prevalent in high-speed optical transmission as a compromise among complexity, transmission bandwidth, and receiver sensitivity, the maximum number of levels for the multi-level delta-sigma IFoF is practically limited to four [8,9,12,13]. Because of this practical limitation, the benefits gained by the multi-level approach are not significant. For example, according to Eq. (1), the amount of quantization noise reduction is only 6 dB when the number of output levels increases from two to four.

Moreover, the sampling frequency of a delta-sigma modulator for optical transmission is usually in the order of GHz or even above 10 GHz for mobile fronthaul applications [8,9], and the multi-level approach with such high sampling frequencies invites several critical problems. One of the issues is the non-linearity of the multi-level quantizer for delta-sigma modulation [14]. Due to the chip foundry process and environmental changes such as temperature fluctuation, the characteristics of both active and passive circuit components vary typically up to ± 20%. That means that the individual amplitude level of feedback DACs in the delta-sigma modulator varies and considerably affects the modulator performance. Figure 3 depicts the simulated signal-to-quantization-noise-ratio (SQNR) of a 4th-order 4-level delta-sigma modulator over variations in the two mid-levels. NTF out-of-band gain of 1.8 and OSR of 12 were used in the evaluation. According to the simulation results, the amount of SQNR degradation is approximately 18 dB, and the maximum SNQR is limited to around 38 dB with the given worst-case non-linearity. The output PSDs for the best and worst cases are depicted in the right-most plot in Fig. 3. Although, in conventional multi-level delta-sigma ADC and DAC applications, dynamic element matching (DEM) logic circuits are used to compensate for the level non-linearity [14], it is hard to apply the technique to delta-sigma IFoF systems because the DEM logic introduces substantial feedback delay at very high-speed sampling frequencies due to its high complexity, which in turn makes the modulator unstable. This is the reason most ultra-high-speed delta-sigma modulators adopt a two-level quantizer [15–17].

Optics EXPRESS

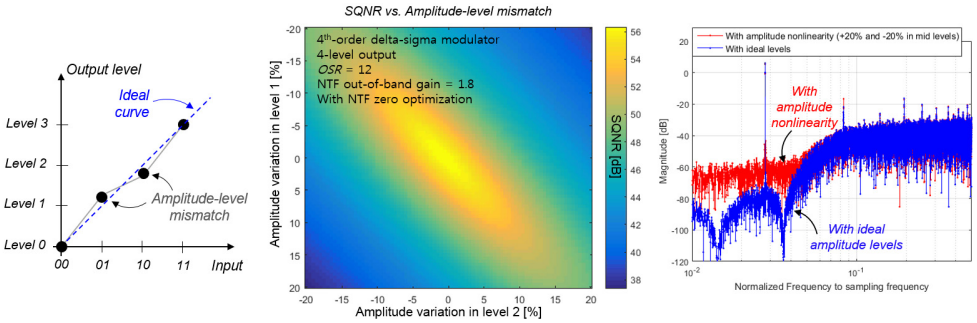

Fig. 3. Simulated SQNRs and PSDs over amplitude mismatch in two mid-levels of a four-level quantizer in a delta-sigma modulator.

3. Proposed correlatively-coded delta-sigma-IFoF system

To mitigate the issues of the conventional delta-sigma IFoF system, we propose a correlative-code-assisted delta-sigma IFoF system. The correlative coding scheme is briefly described first in Section 3.1, and then the proposed architecture is given in Section 3.2.

3.1 Correlative coding

In correlative coding, also known as partial response signaling, a controlled amount of inter-symbol interference (ISI) with the previous K symbols from the present symbol in an input signal is introduced and used to increase the spectral efficiency by creating a correlation between the adjacent signal symbols. The best well-known example of this code is duo-binary signaling [18–20]. The encoder can be implemented with delay-and-add filters as illustrated in Fig. 4, and the output signal is described as

$$y_n = x_n + x_{n-1} + x_{n-2} \cdots + x_{n-K} = \sum_{i=0}^{K} x_{n-K}, \tag{2}$$

where x_n and y_n are the nth input and output symbols of the encoder, respectively. In the encoding process, the nth output symbol y_n is generated by correlating the current nth input symbol x_n and the K previous symbols, which is the reason this encoding is called correlative coding. The correlative encoder can also be implemented in an analog manner with a linear-phase low-pass filter illustrated in Fig. 4(b) [18,19]. The lower the cut-off frequency of the low-pass filter is, the larger ISI occurs. With this characteristic, the amount of ISI can be controlled by adjusting the bandwidth of the filter.

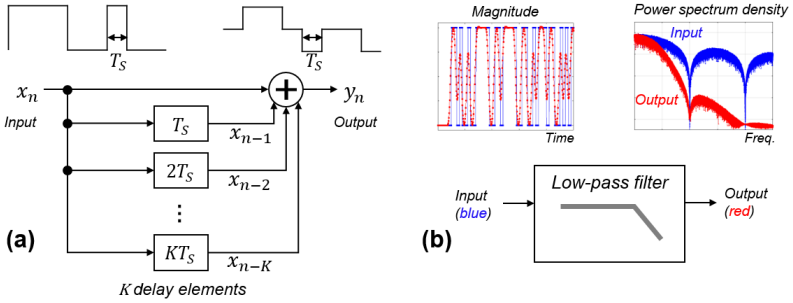

Fig. 4. Correlative encoder implementations: (a) a delay-and-add filter and (b) an analog low-pass filter.

As K increases or the cut-off frequency of the analog low-pass filter decreases, the encoded output pulse waveforms vary more slowly in time because the encoding operation is

Optics EXPRESS

similar to a moving average function. Consequently, the encoder compresses the bandwidth of the input binary signal at the cost of the increased number of output levels.

3.2 Proposed correlatively-coded delta-sigma IFoF system

The architecture and basic operation principle of the proposed correlatively-coded delta-sigma IFoF system are illustrated in Fig. 5. With the proposed two-step coding process comprised of the delta-sigma modulation at a higher sampling rate than the transmission bandwidth, f_s, and the correlative-level encoder that compresses the bandwidth of the delta-sigma digitized signal to the transmission bandwidth of the IFoF system, the proposed scheme shows improved signal quality or higher transmission capacity than the conventional multi-level approach because the quantization noise is more aggressively shaped and moved away from the in-band due to the higher sampling frequency than in the conventional scheme. This is also easily evaluated by the following well-known equation denoting the in-band quantization noise power with an Lth-order NTF of $\left(1-z^{-1}\right)^L$:

$$q_{in-band,RMS}^2 = \frac{\pi^{2L} q_{total,RMS}^2}{(2L+1)OSR^{2L+1}} = \frac{\pi^{2L} q_{total,RMS}^2}{(2L+1)\left(\frac{f_{DSM}}{2BW_{in-band}}\right)^{2L+1}} \tag{3}$$

where OSR is an oversampling ratio defined as $f_{DSM}/(2BW_{in-band})$, f_{DSM} is the sampling frequency for delta-sigma modulation, $BW_{in-band}$ is the in-band signal bandwidth and $q_{total,RMS}^2$ is the total quantization noise power defined in Eq. (1). According to Eqs. (1) and (2), the in-band quantization noise power $q_{in-band,RMS}^2$ is proportional to the square of LSB, Δ^2, and the LSB is determined by the number of output levels. Therefore, as the number of output levels increases by two times, the in-band quantization noise power $q_{in-band,RMS}^2$ is attenuated by a factor of 2^2. However, in Eq. (2), as OSR is doubled with a two-times-higher f_{DSM}, the in-band quantization noise power, $q_{in-band,RMS}^2$, decreases by a factor of 2^{2L+1}, which is undoubtedly a considerable improvement over the factor of 2^2 by the conventional scheme.

Besides, since the proposed scheme uses a two-level quantizer and feedback DACs rather than multi-level circuits, they are intrinsically linear and no amplitude-level-mismatch issue exists, thereby providing stable operation against external influences.

Moreover, compared to a correlative-code-only transmission system, another benefit arises from using the proposed two-step modulation. As shown in Fig. 5, because the original signals are recovered by the filter, a precoder that avoids the error propagation essentially required in conventional correlatively-encoded signaling schemes such as duobinary [20] is not needed in the proposed system. Consequently, if an error exists during the signal reception, it affects only the instantaneous amplitude level during the present symbol time period because it does not propagate from bit to bit.

Optics EXPRESS

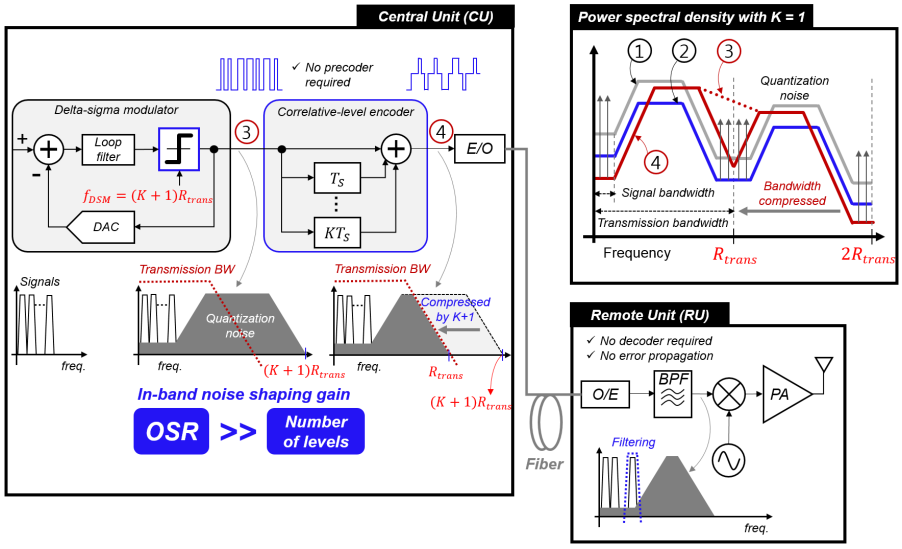

Fig. 5. Block diagram of a proposed correlatively-coded delta-sigma IFoF system and an example of PSDs of signals in the conventional scheme (Fig. 2) and the proposed scheme.

Figure 6 shows the simulated spectra of the conventional 4-level delta-sigma digitized signal and the proposed correlatively-coded delta-sigma modulated signal with K of 1 with the 3-level output (duo-binary). The frequency in the x-axis is normalized to the transmission rate of IFoF systems defined here as R_{trans}. Cascade of integrator with distributed feedback (CIFB) and cascade of resonator with distributed feedback (CRFB) structures with 4th-order NTFs are used without and with the zero optimization technique in the simulation. Regardless of the NTF zero optimization technique, the proposed scheme shows better performance. As clearly seen in Fig. 6, the quantization noise in the proposed system is pushed further away from the in-band, and most of the quantization noise is located at a higher frequency range, as expected. As a result, even though the total amount of quantization noise in the proposed system with 3-level output is larger than that of the 4-level conventional scheme, better in-band signal quality and higher capacity are obtained.

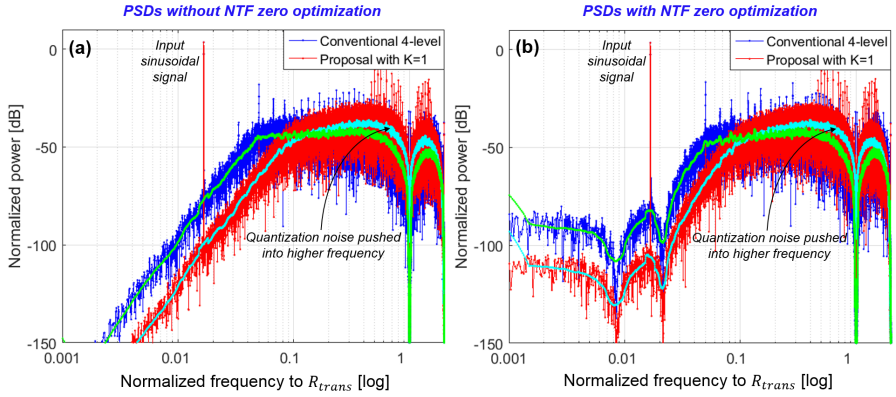

Fig. 6. Simulated PSDs of the conventional 4-level and proposed correlatively-coded delta-sigma-modulated signals (a) without and (b) with NTF zero optimization technique.

To evaluate the extent of the improvement of signal quality and capacity by the proposed scheme, the SQNRs of the conventional 4-level delta-sigma-modulated signal and the proposed correlatively-coded delta-sigma-digitized signals with two different K values of 1

Optics EXPRESS

and 2, were simulated for various $BW_{in-band}$ values normalized to R_{trans}, as shown in Figs. 7(a)-7(c). Fourth–order delta-sigma modulators with different OSRs according to $BW_{in-band}$ were synthesized with the NTF out-of-band gain of 1.8, and their SQNR performance was evaluated over input signal magnitude in dBFS (dB relative to Full Scale) for the simulation. For a more practical evaluation, we applied the NTF zero optimization technique for all the cases. A sinusoidal wave at a frequency of one-eighth of $BW_{in-band}$ was used as an input signal to take into account higher-order harmonics.

In the conventional 4-level delta-sigma case in Fig. 7(a), the peak SQNR for a $BW_{in-band}$ of $0.083R_{trans}$ ($f_{DSM,PAM4} = R_{trans}, OSR \sim 6$) is 35.1 dB. For a similar SQNR performance, the proposed schemes provide a $BW_{in-band}$ up to $0.125R_{trans}$ ($f_{DSM,K=1} = 2\times R_{trans}$, $OSR \sim 8$) and $0.167R_{trans}$ ($f_{DSM,K=2} = 3\times R_{trans}$, $OSR \sim 9$) for K of 1 and 2, respectively. That means, compared with the conventional scheme, the capacity of the proposed system increases by approximately 50% with $K = 1$ and 100% for $K = 2$, which is a significant improvement.

For the same $BW_{in-band}$, higher signal quality can be achieved with the proposed system. With a $BW_{in-band}$ of $0.031R_{trans}$, the maximum SQNR of the conventional 4-level system was 70.0 dB, and with the proposed system, it was 81.8 dB (11.8 dB higher) and 99.1 dB (29.1 dB higher) for K of 1 and 2, respectively. For a $BW_{in-band}$ of $0.083R_{trans}$, the peak SQNR of the conventional approach was 35.1 dB, while the proposed systems provided 47.3 dB (12.2 dB higher) and 60.3 dB (25.2 dB higher) respectively for K of 1 and 2.

Moreover, to find out the impact of the number of order of a delta-sigma modulator, the SQNR performance of the three systems were simulated with 2nd to 5th-order delta-sigma modulators for $BW_{in-band} = 0.083R_{trans}$, as shown in Figs. 7(d)-7(f). Interestingly, it is observed that, the SQNR improvement with a higher order in the conventional 4-level delta-sigma modulator in Fig. 7(d) is apparently small compared to the proposed schemes in Figs. 7(e)-7(f). It is inferred that the negligibly small SQNR improvements are due to the delta-sigma modulator operating less ideally with the much lower OSR of 6. In contrast, the SQNR improvements from 2nd to 5th order in the proposed scheme are approximately 10.9 dB (38.1 dB to 49.0 dB) and 17.3 dB (47.3 dB to 64.6 dB) for K of 1 and 2, respectively.

Overall, in terms of capacity and signal quality, the proposed scheme achieved better performance than the conventional multi-level architecture. However, the proposed system also has disadvantages against the conventional scheme. In Figs. 7(b)-7(c) and 7(e)-7(f), the input magnitudes at peak SQNRs of the proposed scheme were smaller than those of the conventional counterpart. Therefore, a higher gain is necessary to compensate for the lower power of the analog signals in the received modulated pulse waveform at RU. However, the required additional gain for a similar SNQR value is not that large and just less than 6 dB from the simulation results with K up to 2. The received signal power reduction is easily compensated for with an additional gain amplifier with enough gain margin. Another possible drawback of the proposed IFoF system is the requirement of the high sampling-rate delta-sigma modulator. However, with currently available high-speed chip manufacturing processes, the sampling frequency of the delta-sigma modulator can increase up to 50 GHz [15], which is high enough for recent high-speed optical transmission systems. The pros and cons of the proposed and the conventional IFoF systems are summarized in Table 1.

Optics EXPRESS

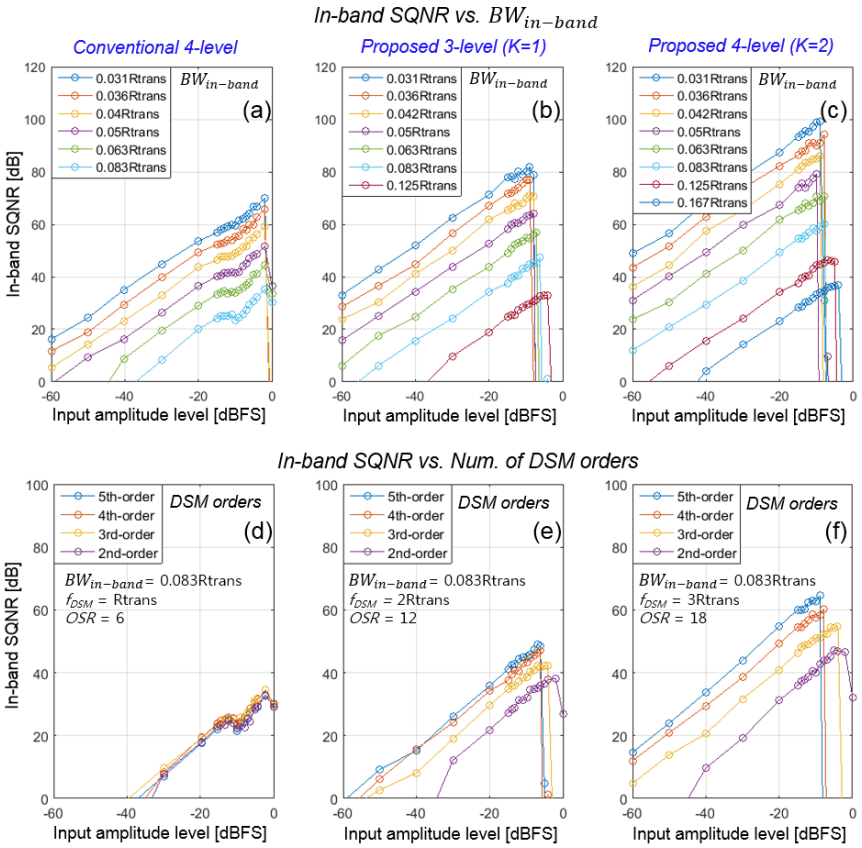

Fig. 7. Simulated SQNRs for various $BW_{in-band}$ with respect to R_{trans}: (a) the conventional 4-level delta-sigma-modulated signal and the proposed correlatively-coded delta-sigma-digitized signals with (b) $K = 1$ and (c) $K = 2$, and simulated SQNRs over the delta-sigma modulator orders from 2nd to 5th: (d) the conventional 4-level and the proposed delta-sigma-digitized signals with (e) $K = 1$ and (f) $K = 2$

Table 1. Pros and cons of the conventional and proposed delta-sigma IFoF systems

	Conventional multi-level delta-sigma IFoF	Proposed correlatively-coded delta-sigma IFoF
Pros	• No additional modulation block required • Higher signal power with higher coding efficiency	• Better in-band signal quality • Larger capacity
Cons	• Poorer in-band signal quality • Smaller capacity • Higher amplitude-level non-linearity	• Lower signal power • Higher-speed delta-sigma modulator circuit required

4. Experimental setup and results

The proposed correlative-code-assisted delta-sigma IFoF system is experimentally evaluated with multiple LTE signals with a modulation format of 64 quadrature amplitude modulation (QAM). For comparison, two PAM-4-based delta-sigma-digitized IFoF systems were also implemented and demonstrated with the same optical link.

4.1 Experimental setup

The experimental setup for an evaluation of the three delta-sigma-IFoF systems is depicted in Fig. 8. Multiple LTE 10 MHz IF signals with 64 QAM were generated in the LTE signal

Optics EXPRESS

generator. Due to the lack of a high-speed signal generator and analyzer, the sampling frequencies of the delta-sigma modulator for the proposed and the conventional PAM-4 IFoF schemes have been selected as 2 GHz for $K=1$ ($f_{DSM,K=1}=2\times R_{trans}$) and 1 GHz ($f_{DSM,PAM4}=R_{trans}$), respectively, for transmission bandwidth of R_{trans} = 1 GHz. It is noted that R_{trans} = 1 GHz is not the 3-dB bandwidth of the transmission system in the experimental setup. The 3-dB bandwidth of the system is mainly determined by a 5th-order low-pass Bessel filter with a 3-dB cut-off frequency of 800 MHz. The filter operates as an analog correlative encoder for the proposed scheme and a transmit channel filter for conventional PAM-4 systems.

For signal digitation, fourth-order low-pass delta-sigma modulators were designed by a signal processing software to convert the multi LTE 10 MHz IF signals into two- or four-level delta-sigma-modulated signals. The LTE signals applied to the delta-sigma modulators were centered at 5 MHz and 95 MHz for the first and last channels, respectively, and the total signal bandwidth was 100 MHz (total 10 LTE channels).

Because it was expected that the error-vector-magnitude (EVM) performance of the PAM-4 delta-sigma-IFoF system with 10 LTE channels would be poorer than that of the proposed IFoF system due to low *OSR* values, another four-level delta-sigma-IFoF link for seven LTE channels (lower signal bandwidth and then higher OSR, which results in better signal quality) was developed, shown in the bottom path in the transmitter side in Fig. 8.

The delta-sigma-digitized output bits from the three paths were then delivered to the pulse pattern generators (PPGs) (Agilent E4862B), PPG #1 to #3. All PPGs were controlled to provide the same amplitude level of 1 Vpp (peak-to-peak voltage) at their output. For the proposed IFoF in the top path, the two-level output pulse of PPG #1 is applied to the 5th-order Bessel duo-binary filter with a bandwidth of 800 MHz to generate a three-level correlative pulse train from the 2-level input pulse train by reducing the signal bandwidth. The three-level correlative-coded delta-sigma-digitized multi-IF LTE signal was then transmitted over the 10 km fiber by an SFP optical transmitter with a C-band distributed feedback laser supporting up to 3.1 Gbps transmission, and detected by the PIN PD with TIA at the receiver side. The other two PAM-4 delta-sigma-IFoF signals are applied to the multi-level optical transmitter through the channel filters (the same filter used in the proposed link, the 5th-order 800 MHz-bandwidth Bessel filter) to ensure all the signals in the three different paths in Fig. 8 experience the same frequency response for proper comparison.

The signals were received at the PD and captured by an oscilloscope (Keysight DSO-S 204A) with a capture bandwidth of 2 GHz for the bit error rate (BER) evaluation and the operations of the clock-and-data recovery (CDR). The captured waveforms were then reconstructed as digital pulse trains by another PPG (Agilent E4862B), PPG #4. For the proposed and conventional PAM-4 delta-sigma-IFoF links, the received signals were quantized respectively into three and four levels. With the CDR and the DAC (PPG #4), most of distortions and noise present in the received digital signals at the O/E converter could be removed out. As a result, clear rectangular pulse waveforms were obtained at the PPG #4 output. This operation, named here as pulse recovery, is essential because the bit streams from the delta-sigma modulators at transmitter side were generated based on an ideal rectangular pulse shape (more strictly, the pulse shape of the feedback DACs in the delta-sigma modulators), and any discrepancies between the received pulse waveform and the ideal rectangular waveform decreased the SNR. However, because the impacts of non-ideal pulse shapes and jitter by PPG#4 on the in-band signal quality cannot be compensated, they were taken account of in the present evaluation.

The reconstructed multi-level signals were finally sampled by DSO (Keysight DSO-S 204A) to be analyzed in the multi-IF LTE signal analyzer. In this analysis stage, further quantization operation making the received pulse waveforms more ideal was not conducted,

Optics EXPRESS

and the non-idealities by the PPGs are taken into account. The important parameters for the experimental setup are summarized in Table 2.

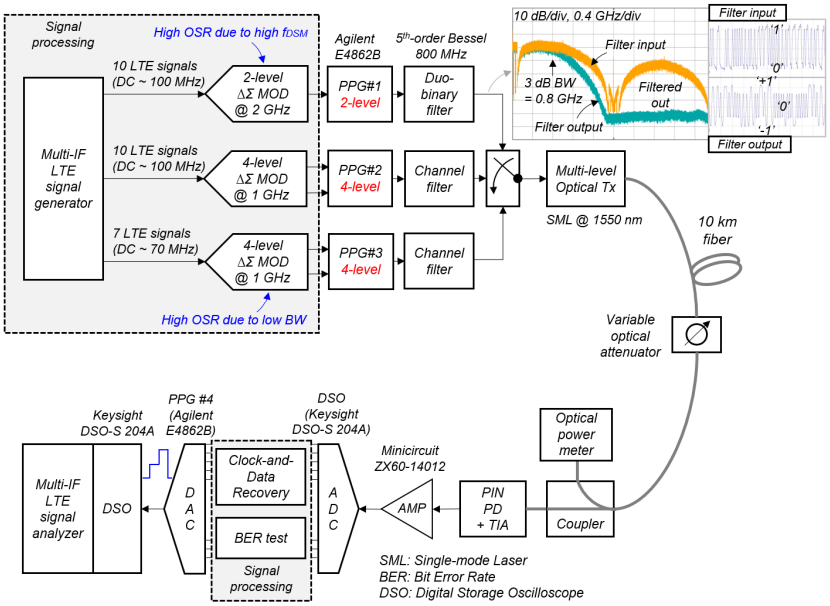

Fig. 8. Experimental setup for the conventional multi-level delta-sigma-IFoF and proposed correlatively-coded IFoF systems.

Table 2. Important parameters of the two different conventional delta-sigma IFoF systems with PAM-4 and the proposed correlatively-coded IFoF system in the experimental setup

Architecture	NTF (Z-domain)	NTF order	Num. levels (DSM)	f_{DSM}	Num. levels (Transmission)	R_{trans}
Conventional PAM-4 10 Channels	$\frac{(z^2-1.953z+1)(z^2-1.703z+1)}{(z^2-1.054z+0.2949)(z^2-1.246z+0.5863)}$	4	4	1 GHz	4	1 GHz
Conventional PAM-4 7 Channels	$\frac{(z^2-1.976z+1)(z^2-1.85z+1)}{(z^2-1.253z+0.4059)(z^2-1.483z+0.6809)}$	4	4	1 GHz	4	1 GHz
Proposed Duo-binary 10 Channels	$\frac{(z^2-1.988z+1)(z^2-1.924z+1)}{(z^2-1.284z+0.4249)(z^2-1.515z+0.695)}$	4	2	2 GHz	3 (duo-binary)	1 GHz

4.2 Experimental results and discussions

The measured BER curves of the three IFoF systems versus the received optical power are depicted in Fig. 9(a). Because the duo-binary–encoded delta-sigma-IFoF has three levels while the PAM-4 delta-sigma-IFoF links have four levels, the proposed IFoF scheme had better vertical eye-opening, leading to higher optical power margin. According to [12], the duo-binary signaling scheme has a 2.8 dB better optical power margin over PAM-4. It is well matched with the measured power margin of higher than 2 dB.

The measured eye diagrams at various received power levels are also shown in Figs. 9(b) to 9(j) for the duo-binary delta-sigma-IFoF link with 10 LTE channels and the two PAM-4 delta-sigma-IFoF systems with 10 and 7 LTE signals.

Optics EXPRESS

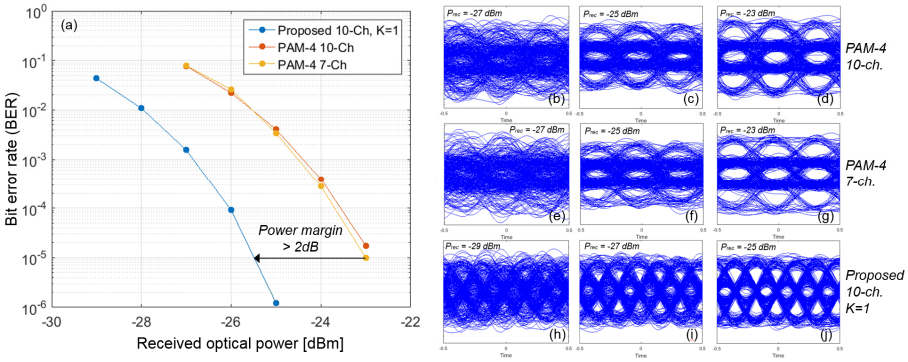

Fig. 9. Measured BER and eye diagrams: (a) BER, and eye diagrams of the conventional PAM-4 10-channel IFoF at (b) P_{rec} = –27 dBm, (c) P_{rec} = –25 dBm and (d) P_{rec} = –23 dBm, and eye diagrams of the conventional PAM-4 7-channel IFoF at (e) P_{rec} = –27 dBm, (f) P_{rec} = –25 dBm and (g) P_{rec} = –23 dBm, and eye diagrams of the proposed 10-channel IFoF with K = 1 at (h) P_{rec} = –29 dBm, (i) P_{rec} = –27 dBm and (j) P_{rec} = –25 dBm .

To elucidate the spectral behaviors of the proposed correlative-code-assisted delta-sigma-IFoF and the conventional PAM-4 delta-sigma-IFoF systems, the measured received signal spectra of the PD and CDR (PPG #4) outputs are depicted in Figs. 10(a) to 10(f). Because f_{DSM} in the proposed delta-sigma-IFoF system was 2 GHz, the replica of the LTE signals was observed at 2 GHz, as depicted in Fig. 10(f); whereas, in the two PAM-4 delta-sigma-IFoF systems, the 1st replicas of the LTE signals were at 1 GHz, clearly seen in Figs. 10(d) and 10(e). In Figs. 10(c) and 10(f), the spectral shapes of the two signals are quite different. This is because the hybrid CDR output signal is reconstructed in the form of a 3-level rectangular pulse by the pulse recovery, described in the experimental setup in Section 4.1, while the duo-binary-encoded signal is generated by the analog version of the correlative encoding with the Bessel filter at the transmitter side. As clearly seen in Fig. 10, with the pulse recovery operation, most of the distortions and noise from the optical link were attenuated out, and thus the reconstructed signals had higher SNRs than those at PD outputs. In the proposed IFoF in Figs. 10(c) and 10(f), the observed pulse recovery gain was approximately 15 dB (from 17 dB to 32 dB). This advantage can be used repeatedly along a transmission system with amplitude-level quantizers. Thanks to the digital signaling scheme.

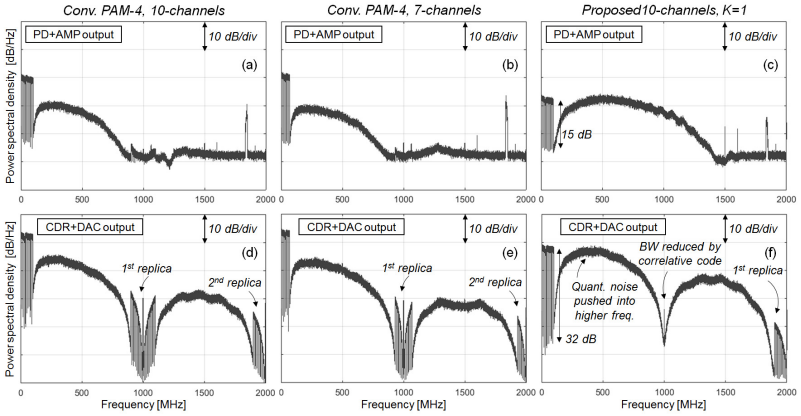

Fig. 10. Measured received signal spectra at the PD of the (a) PAM-4, 10-Ch, (b) PAM-4, 7-Ch, and (c) proposed 10-Ch K = 1, and the measured signal spectra at the CDR of (d) PAM-4, 10-Ch, (e) PAM-4, 7-Ch, and (f) proposed 10-Ch K = 1 IFoF systems.

Optics EXPRESS

To evaluate the BER tolerance of the three delta-sigma IFoF systems, the EVM performance over various BER values with different received optic power levels were measured, and are depicted in Figs. 11(a)-11(c). Due to the limited memory size of the PPG and the DSO used in the experimental setup, the capture time period for the analysis is also limited, and as a result, the minimum BER to be measurable was ~ 1×10^{-6}. Therefore, the error-free transmissions were observed at the received optical powers of –22 dBm and –24 dBm for the two conventional and proposed IFoF systems, respectively. Again, this additional power margin for the same BER performance was originated from the fact that the proposed scheme has the lower number of signal levels than the conventional counterpart, as illustrated in Fig. 9(a). According to the experimental results in Fig. 11, the BER threshold values for 3GPP LTE 64 QAM requirement of EVM 8% were approximate to 3.9×10^{-4}, 3.4×10^{-3} and 1.5×10^{-3}, respectively, for the PAM-4 10-channel, PAM-4 7-channel and proposed duo-binary 10-channel IFoF systems.

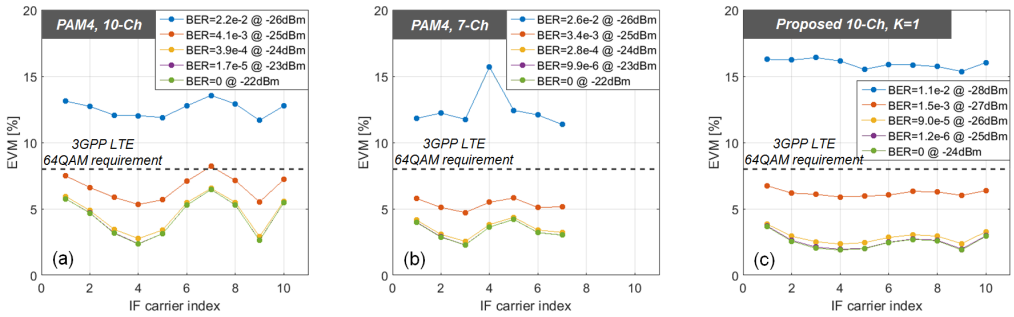

Fig. 11. Measured EVM values of the (a) PAM-4, 10-Ch, (b) PAM-4, 7-Ch, and (c) proposed 10-Ch $K = 1$ IFoF systems.

The measured best-case EVM values over IF channels of the three IFoF systems are also shown in Fig. 12(a). In the proposed delta-sigma-IFoF system, the measured best-case EVMs were all less than 3% except the first channel, 3.7%. However, the 10-channel PAM-4 delta-sigma-IFoF showed the best-case EVM values up to 6.5% with a small margin of 1.5% for the 3GPP LTE 64-QAM requirement. For the 7-channel PAM-4 delta-sigma-IFoF, the amount of the in-band quantization noise was lower than that of the 10-channel system, as designed, and its measured best-case EVM performance was similar to that of the proposed duobinary IFoF. The measured maximum best-case EVM in 7-channel PAM-4 IFoF was 4.2% at IF carrier index #5.

From the measurement results, the capacity of the proposed correlatively-encoded delta-sigma-IFoF system with 10 LTE channels was approximately 40% higher than that of the PAM-4 7-channel delta-sigma-IFoF with 7 LTE channels for the same signal quality. This increase in capacity was obtained even at 2 dB lower received optical power. For the evaluation of the signal quality improvement, the EVM performances of the PAM-4 IFoF and the proposed IFoF links were compared. Average EVM improvement between the two systems was ~2.1%, whereas the maximum EVM enhancement of 3.8% (6.5% for PAM-4, 2.7% for proposed duo-binary) was observed at IF carrier index #7. The measured LTE 64-QAM constellations of the three systems at the best-case transmissions are also illustrated in Fig. 12(b).

Optics EXPRESS

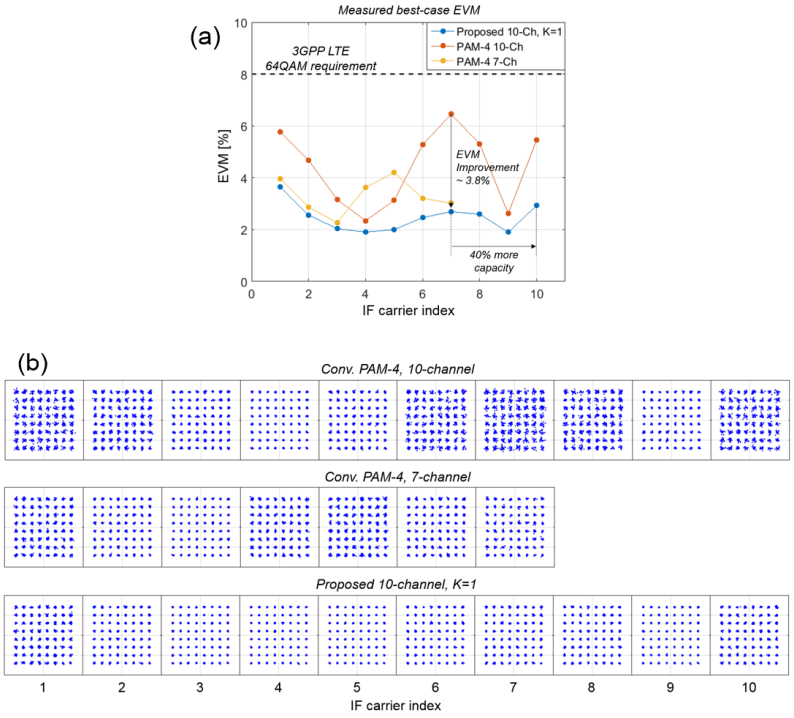

Fig. 12. Measured best-case signal performance: (a) EVM values of the two PAM-4 systems with 7-Ch and 10-Ch and the proposed 10-Ch K = 1 IFoF system, and (b) the IF-carrier constellations for the three IFoF systems

For an evaluation of the overall system performance, the measured average EVM values with respect to received optic power levels and the relation between the average EVM and BER of the three IFoF systems are shown in Fig. 13. As described, the additional optic power margin of ~2 dB due to the lower number of quantization levels of the proposed scheme is clearly observed in Fig. 13(a). At the received optic power levels of > –27 dBm, the average EVM values of the proposed link satisfied the 3GPP LTE EVM requirement of 8%. In the case of the two PAM-4 IFoF systems, the threshold of the receiver optic power was –25 dBm. The minimum average EVM for the PAM-4 10-channel/7-channel IFoF and the proposed 10-channel IFoF systems were 4.6%, 3.4%, and 2.5%, respectively.

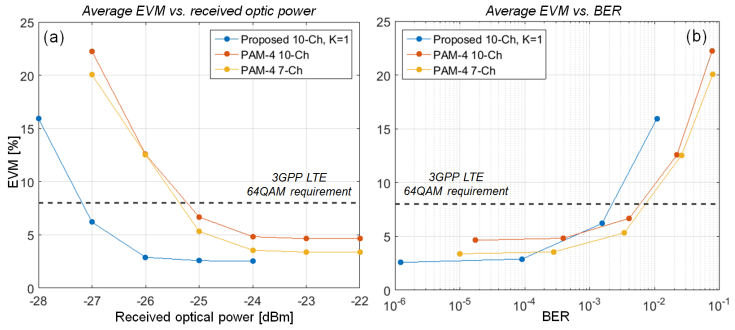

Fig. 13. Measured overall performance of the two PAM-4 systems with 7-Ch and 10-Ch and the proposed 10-Ch K = 1 IFoF system: (a) measured average EVM values against receiver optic power levels and (b) measured average EVM values over BER.

Optics EXPRESS

5. Conclusion

In this paper, we proposed and verified a correlatively-coded delta-sigma IFoF transmission system in which the sampling frequency for delta-sigma modulation can increase beyond the transmission bandwidth. For experimental evaluation, 10 LTE 10 MHz IF signals were first delta-sigma digitized with two levels at 2 GHz, and then correlatively coded with $K=1$, which resulted in a three-level pulse train with an 800 MHz 5th-order Bessel low-pass filter to be transmitted over an IFoF link with R_{trans} = 1GHz. We also demonstrated two more conventional 4-level delta-sigma IFoF links with 10 and 7 IF channels at f_{DSM} = 1GHz for PAM-4 transmission for comparative analysis in capacity and signal quality.

Compared to the conventional PAM-4 systems, the proposed method provides at least 40% larger transmission capacity for similar in-band signal quality and, at the same time, shows 2 dB better receiver sensitivity with three output signaling levels ($K=1$). In terms of signal quality with the same capacity, the proposed link shows 2.1% better average EVM performance and a maximum EVM improvement of 3.8% (6.5% for PAM-4, 2.7% for proposed duo-binary) at IF carrier index #7.

Based on the evaluation results, the proposed IFoF system increases the transmission capacity, provides higher power margins or improves the in-band signal fidelity. Due to the high spectral efficiency, the proposed scheme requires the lowest transmission capacity per LTE signal among delta-sigma-based IFoF systems up to date. Moreover, the anticipated improvements in capacity and signal quality in the proposed system become considerably bigger with a higher K, which is favorable to the next-generation high-capacity mobile signal transmission systems.

Funding

Institute for Information & communications Technology Promotion (IITP) grant funded by the Korea government (MSIT) (2017-0-00409, Development on millimeter-wave beamforming IC for 5G mobile communication).

References

1. X. Liu, F. Effenberger, N. Chand, L. Zhou, and H. Lin, " Demonstration of bandwidth-efficient mobile fronthaul enabling seamless aggregation of 36 E-UTRA-like wireless signals in a single 1.1-GHz wavelength channel," in *Optical Fiber Communication Conference* (Optical Society of America, 2015), paper M2J–2.
2. B. G. Kim, H. Kim, and Y. C. Chung, "Impact of Multipath Interference on the Performance of RoF-Based Mobile Fronthaul Network Implemented by Using DML," J. Lightwave Technol. **35**(2), 145–151 (2017).
3. J. Wang, C. Liu, J. Zhang, M. Zhu, M. Xu, F. Lu, L. Cheng, and G.-K. Chang, "Nonlinear inter-band subcarrier intermodulations of multi-RAT OFDM wireless services in 5G heterogeneous mobile fronthaul networks," J. Lightwave Technol. **34**(17), 4089–4103 (2016).
4. S. Jang, C. S. Lee, D. M. Seol, E. S. Jung, and B. W. Kim, "A bidirectional RSOA based WDM-PON utilizing a SCM signal for down-link and a baseband signal for up-link," in *Optical Fiber Communication Conference* (Optical Society of America, 2007), paper jThA78.
5. L. Breyne, G. Torfs, X. Yin, P. Demeester, and J. Bauwelinck, "Comparison Between Analog Radio-Over-Fiber and Sigma Delta Modulated Radio-Over-Fiber," IEEE Photonics Technol. Lett. **29**(21), 1808–1811 (2017).
6. S. Jang, G. Jo, J. Jung, B. Park, and S. Hong, "A digitized IF-over-fiber transmission based on low-pass delta-sigma modulation," IEEE Photonics Technol. Lett. **26**(24), 2484–2487 (2014).
7. A. Kanno and T. Kawanishi, "Analog signal transmission by FPGA-based pseudo-delta-sigma modulator," in *IEEE Photonics Conference* (IPC, 2015), pp. 136–137.
8. J. Wang, Z. Yu, K. Ying, J. Zhang, F. Lu, M. Xu, L. Cheng, X. Ma, and G. K. Chang, "10-Gbaud OOK/PAM4 digital mobile fronthaul based on one-bit/two-bit Δ-Σ modulation supporting carrier aggregation of 32 LTE-A signals with up to 256 and 1024QAM," in *42nd European Conference on Optical Communication* (Optical Society of America, 2016), paper W.4.P1.SC7.68.
9. H. Li, R. Hu, Q. Yang, M. Luo, Z. He, P. Jiang, Y. Liu, X. Li, and S. Yu, "Improving performance of mobile fronthaul architecture employing high order delta-sigma modulator with PAM-4 format," Opt. Express **25**(1), 1–9 (2017).
10. C. Li, R. Hu, H. B. Li, M. Luo, Q. Yang, and S. Yu, "Digital OFDM-PON Based on Delta–Sigma Modulation Employing Binary IM-DD Channels," IEEE Photonics J. **9**(2), 1–7 (2017).

Optics EXPRESS

11. S. Jang, B. Park, and S. Hong, "Digital radio-over-fiber system with multi-pulse Manchester encoding-assisted delta-sigma modulation," Opt. Express **25**(7), 8335–8349 (2017).
12. J. Wang, Z. Jia, L. Campos, L. A. Cheng, C. Knittle, and G. K. Chang, "Delta-Sigma Digitization and Optical Coherent Transmission of DOCSIS 3.1 Signals in Hybrid Fiber Coax Networks," J. Lightwave Technol. **36**(2), 568–579 (2018).
13. J. Wei, N. Eiselt, H. Griesser, K. Grobe, M. Eiselt, J. J. Vegas-Olmos, and J. P. Elbers, "First demonstration of real-time end-to-end 40 Gb/s PAM-4 system using 10-G transmitter for next generation access applications," in *European Conference on Optical Communication* (Optical Society of America, 2015), paper PDP 4.4.
14. A. Sanyal, L. Chen, and N. Sun, "Dynamic Element Matching with Signal-Independent Element Transition Rates for Multibit ΔΣ Modulators," IEEE Trans. Circuits Syst. I Regul. Pap. **62**(5), 1325–1334 (2015).
15. A. Hart and S. P. Voinigescu, "A 1 GHz Bandwidth Low-Pass ΔΣ ADC With 20–50 GHz Adjustable Sampling Rate," IEEE J. Solid-State Circuits **44**(5), 1401–1414 (2009).
16. T. Chalvatzis, E. Gagnon, M. Repeta, and S. P. Voinigescu, "A Low-Noise 40-GS/s Continuous-Time Bandpass ΔΣ ADC Centered at 2 GHz for Direct Sampling Receivers," IEEE J. Solid-State Circuits **42**(5), 1065–1075 (2007).
17. B. Park, S. Jang, P. Ostrovskyy, and J. Jung, "A high voltage swing dual-band bandpass modulator for mobile base-station," IEEE Microw. Wirel. Compon. Lett. **23**(4), 199–201 (2013).
18. C. Sun, S. H. Bae, and H. Kim, "Transmission of 28-Gb/s duobinary and PAM-4 signals using DML for optical access network," IEEE Photonics Technol. Lett. **29**(1), 130–133 (2017).
19. M. Rannello, M. Presi, and E. Ciaramella, "Optical vs. Electrical Duobinary Coding for 25 Gb/s PONs based on DSP-free Coherent Envelope Detection," in *Optical Fiber Communication Conference* (Optical Society of America, 2018), paper M1B.6.
20. J. Lee, M. S. Chen, and H. D. Wang, "Design and comparison of three 20-Gb/s backplane transceivers for duobinary, PAM4, and NRZ data," IEEE J. Solid-State Circuits **43**(9), 2120–2133 (2008).